AUTHOR QUERY FORM

ELSEVIER	**Journal:** AESCTE **Article Number:** 3491	**Please e-mail your responses and any corrections to:** **E-mail:** corrections.esch@elsevier.vtex.lt

Dear Author,

Please check your proof carefully and mark all corrections at the appropriate place in the proof (e.g., by using on-screen annotation in the PDF file) or compile them in a separate list. Note: if you opt to annotate the file with software other than Adobe Reader then please also highlight the appropriate place in the PDF file. To ensure fast publication of your paper please return your corrections within 48 hours.

For correction or revision of any artwork, please consult *http://www.elsevier.com/artworkinstructions*

Any queries or remarks that have arisen during the processing of your manuscript are listed below and highlighted by flags in the proof. Click on the 'Q' link to go to the location in the proof.

Location in article	Query / Remark: click on the Q link to go Please insert your reply or correction at the corresponding line in the proof
Q1	Your article is registered as a regular item and is being processed for inclusion in a regular issue of the journal. If this is NOT correct and your article belongs to a Special Issue/Collection please contact <a.stanly@elsevier.com> immediately prior to returning your corrections. (p. 1/ line 1)
Q2	Please confirm that given names and surnames have been identified correctly and are presented in the desired order. (p. 1/ line 14)
Q3	Please provide a conflict of interest statement. If there is no conflict of interest, state that. (p. 7/ line 97)
Q4	Please check and correct the section number - there is no Section 7 in this article. (p. 1/ line 128)
Q5	Please check the phrase "...differences between a microphone array [3,5], the..." for clarity, and correct if necessary. (p. 1/ line 51)

Please check this box if you have no corrections to make to the PDF file ☐

Aerospace Science and Technology ••• (••••) •••–•••

Contents lists available at ScienceDirect

Aerospace Science and Technology

www.elsevier.com/locate/aescte

Aircraft localization using a passive acoustic method. Experimental test

Sara R. Martín [a,*], Meritxell Genescà [b], Jordi Romeu [a], Arnau Clot [a]

[a] Laboratory of Acoustics and Mechanical Engineering (LEAM), Universitat Politècnica de Catalunya, C/Colom 11, 08222 Terrassa, Spain
[b] Acoustics Research Centre, Department of Electronics and Telecommunications, Norwegian University of Science and Technology, Trondheim, Norway

ARTICLE INFO

Article history:
Received 23 January 2015
Received in revised form 17 August 2015
Accepted 13 November 2015
Available online xxxx

Keywords:
Aircraft
Localization
Wideband cross ambiguity function
Acoustical Doppler effect

ABSTRACT

A passive acoustic method for aircraft localization is experimentally tested in this paper. The method relies on the Doppler effect influencing the signals received by a mesh of microphones distributed over the acoustic area of interest. The relative Doppler stretch factors between the microphone signals are estimated using a one-dimensional version of the Ambiguity function. Then, a Genetic Algorithm is used to solve the non-linear system of equations that relates the aircraft's position and velocity to this relative stretch factors. This method is used in this study to locate a radio controlled airplane equipped with a Global Positioning System (GPS). Seven microphones are distributed in the airfield area. Although the localization errors are influenced by the uncertainty in the microphones position, the acoustic system succeeds at locating the airplane.

1. Introduction

The interest in passive acoustic aircraft localization systems arises when the performance of RADAR systems is reduced such as non-line-of-sight tracking or when electromagnetic radiation is present. Acoustic aircraft localization systems can also be a cheaper alternative in small airports and, in addition, the data from the acoustic sensors can also be processed for source classification or noise monitoring purposes.

Several acoustic methods have been developed to determine the motion parameters such as height and speed of both jet and propeller driven aircraft flying in a straight line at constant flight level and speed. The methods developed for propeller driven aircraft take advantage of the Doppler effect and require one single microphone [1–3] or a distributed array of microphones [4]. The methods developed for jet aircraft use the time differences between a microphone array [3,5], the interference between the direct and ground reflected sounds [6,7] or both [8].

Other techniques are used for the 3D localization of maneuvering aircraft without limitations on the trajectory. For a low altitude aircraft, the sound wavefronts can be considered spherical and the bearing and distance of the aircraft can be estimated with a planar microphone array [9]. At larger distances, the front waves become planar and only the bearing can be obtained with a microphone array. Under these circumstances, a possible approach is to use a distributed network of nodes – a node being in this context a single acoustic sensor or a set of several acoustic sensors – where every node provides an estimate of the aircraft bearing. The 3D position of the aircraft can be calculated afterwards by triangulation of the bearing estimates from, at least, two nodes. Such an approach has the benefit that only the bearing data has to be transmitted to a central processing unit, but the disadvantage is that the nodes are complex systems such as microphone arrays [10–13] or, more recently, acoustic vector sensors [14].

An alternative approach to passive acoustic 3D localization that uses a network of single microphones was initially described in [15,16]. The methods were based on the estimation of time delay between the signals at the different microphones, and therefore they only obtain the bearing of the aircraft.

In contrast, the method used in the present paper relies on both the time delay (retardation effect) and the time stretch (Doppler effect) [17,18] to obtain the source position and velocity. Seven microphones are distributed on the ground within the acoustic area of influence of the moving sound source. This acoustic method for aircraft localization is experimentally tested in this paper.

The rest of the paper is organized as follows. Section 2 describes the acoustic localization method, Section 3 presents the experimental setup, Section 4 describes the parameters used in the implementation of the algorithm for the test, Section 5 shows the experimental results, Section 6 discusses different sources of errors, and finally Section **??** summarizes the main findings of this paper.

* Corresponding author.
E-mail address: sara.martin@upc.edu (S.R. Martín).

http://dx.doi.org/10.1016/j.ast.2015.11.023
1270-9638/

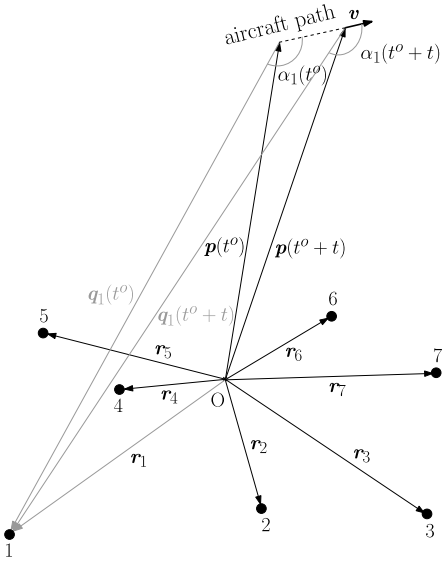

Fig. 1. Microphone set up and geometric variables relevant to the localization algorithm.

2. Localization algorithm

This section describes the localization algorithm and its implementation. Further details of the theoretical background can be found in [17] and [19].

The method requires at least seven microphones randomly distributed as showed in Fig. 1. Their positions $\boldsymbol{r}_n$ for $n \in \{1, .., 7\}$ with respect to an origin $O = [0, 0, 0]$ need to be known.

Let $s_e(t^o + t)$ be the signal emitted by the aircraft t seconds after a certain time t^o, this signal is received at the microphone n at the time $t^o + t'$, which accordingly to Fig. 1 is

$$t' = t + \frac{|\boldsymbol{q}_n(t^o + t)|}{c}, \tag{1}$$

where c is the sound speed in an isospeed medium and $|\boldsymbol{q}_n(t^o + t)| = |\boldsymbol{r}_n - \boldsymbol{p}(t^o + t)|$ is the position vector from the source to the receiver as shown in Fig. 1.

If t is so small that, during the interval $[t^o; t^o + t]$, the distance traveled by the aircraft is much smaller than the distance between the aircraft and the receiver and also the aircraft velocity $\boldsymbol{v}$ can be considered a constant, then the relationship between the received and the emitted signal is [18]

$$y_n(t^o + t') = \rho_n \cdot s_e(t^o + [t' - \frac{|\boldsymbol{q}_n(t^o)|}{c}] \cdot [\frac{c}{c - |\boldsymbol{v}| \cos(\alpha_n(t^o))}]), \tag{2}$$

where y_n corresponds to the acoustic signal received by the n-th microphone, ρ_n represents the amplitude attenuation factor due to the sound propagation and α_n is the angle between the aircraft velocity $\boldsymbol{v}$ and the pathlength vector $\boldsymbol{q}_n$ pointing from the aircraft to the receiver n.

The term $\frac{|\boldsymbol{q}_n(t^o)|}{c}$ in Eq. (2) is the time that the signal takes to propagate from the initial position of the source to the receiver, and the term $\frac{c}{c - |\boldsymbol{v}| \cos(\alpha_n(t^o))}$ is the Doppler effect due to the movement of the source called further on absolute Doppler stretch δf_n. Therefore, the received signal y_n at a microphone n is the emitted signal s_e shifted in time by the propagation time $\frac{|\boldsymbol{q}_n(t^o)|}{c}$ and also stretched – i.e. expanded or contracted – in time by the Doppler effect term $\frac{c}{c - |\boldsymbol{v}| \cos(\alpha_n(t^o))}$. By recursion, it can be easily shown that the signals received at two different microphones are time shifted and time stretched to each other disregarding the amplitude.

The underlying idea of this localization method is that, since the Doppler stretch term is related to the speed and position of the aircraft, if the value of the Doppler stretch could be estimated by comparing the signals of the different microphones, the aircraft could be localized.

The method is iterative, and for each iteration $k \in \mathbb{N}^*$ the initial position $\boldsymbol{p}(t^o)$ of the aircraft at a time t^o needs to be known from the previous iteration. To initialize the method it is necessary that the real position of the aircraft is known at an arbitrary time. Let $\boldsymbol{p}^{\text{initial}}$ at $t^{\text{initial}} = 0$ s be a known value such that

$$t^o = (k-1)\frac{\Delta t}{2}$$

$$\boldsymbol{p}(t^o) = \begin{cases} \boldsymbol{p}^{\text{initial}} & \text{if } k = 1, \\ \boldsymbol{p}^{k-1} & \text{if } k \neq 1. \end{cases} \tag{3}$$

where Δt is the time interval between two successive position estimates, and $\boldsymbol{p}^{k-1}$ is the position estimate obtained in the previous iteration.

The following steps are repeated in each iteration.

Step 1: Signals synchronization

This step consists in selecting the signal portion $x_n(t')$ of every receiver signal $y_n(t^o + t')$ originated when the source was at position $\boldsymbol{p}(t^o)$ and lasting for Δt. The signal originated at $\boldsymbol{p}(t^o)$ reaches the receiver n after a time period $\frac{|\boldsymbol{q}_n(t^o)|}{c} = \frac{|\boldsymbol{r}_n - \boldsymbol{p}(t_o)|}{c}$. Therefore the set of synchronized signal portions $x_n(t')$ are obtained as

$$x_n(t') = y_n(t^o + (t' + \frac{|\boldsymbol{q}_n(t^o)|}{c})) \text{ with } t' \in [0; \Delta t]. \tag{4}$$

Combining Eq. (2) into Eq. (4) it comes out that the relation between the synchronized signal portions and the emitted signal is

$$x_n(t') = \rho_n \cdot s_e(t^o + [\frac{c}{c - |\boldsymbol{v}| \cos(\alpha_n(t^o))}]t'). \tag{5}$$

Eq. (5) shows that the set of synchronized signal portions are time stretched and attenuated versions of each other.

Step 2: Computation of the relative Doppler Effect

This step consists of the calculation of the relative Doppler stretch δf_{mn} between each pair of synchronized signal portions received at microphones m and n. Since

$$\delta f_{mn} = \frac{c - |\boldsymbol{v}| \cdot \cos(\alpha_n(t^o))}{c - |\boldsymbol{v}| \cdot \cos(\alpha_m(t^o))}, \tag{6}$$

the search domain can be limited to

$$\frac{c - |v_{max}|}{c + |v_{max}|} \leq \delta f \leq \frac{c + |v_{max}|}{c - |v_{max}|}, \tag{7}$$

where $|v_{max}|$ is the maximum possible speed reached by the aircraft.

To obtain the value of δf_{mn}, first the discrete Fourier transform $X_n(f)$ of $x_n(t')$ is calculated for all the receivers. Note that both t' and f are discrete variables since $x_n(t')$ is a digital signal. Second, the following discrete 1-dimensional version of the ambiguity function is calculated over a set of attempted relative Doppler stretches δf

$$\chi(\delta f) = \frac{\sqrt{\delta f}}{L+1} \sum_{l=0}^{L} |X_n(l \cdot \Delta f)| \cdot |X_m(\delta f \cdot l \cdot \Delta f))| \tag{8}$$

where L is the available number of frequency bins. Since the Nyqvist theorem predicts that spectral information is limited up to half the sampling frequency f_m, then

$$L = \begin{cases} \left\lfloor \dfrac{f_m/2 \cdot \delta f}{\Delta f} \right\rfloor & \text{if } \delta f < 1, \\ \left\lfloor \dfrac{f_m/2}{\Delta f} \right\rfloor & \text{if } \delta f \geq 1. \end{cases}$$

where Δf is the frequency resolution of the frequency spectra $X_n(f)$.

The ambiguity function in Eq. (6) reaches its absolute maximum value at $\delta f = \delta f_{mn}$ since the frequency spectra satisfy $|X_n(f)| = \gamma_{mn}|X_m(f \cdot \delta f_{mn}))|$ for an amplitude factor γ_{mn}. Therefore, the relative Doppler stretch δf_{mn} between the signals at two different microphones can be deduced as the argument of the maximum of Eq. (8).

Step 3: Calculation of the position estimate

The third step is to obtain an estimate of the aircraft position from the relative Doppler stretch estimates. Eq. (6) can alternatively be expressed as

$$\delta f_{mn} = \frac{c - \dfrac{\boldsymbol{v} \cdot (\boldsymbol{r}_n - \boldsymbol{p})}{|\boldsymbol{r}_n - \boldsymbol{p}|}}{c - \dfrac{\boldsymbol{v} \cdot (\boldsymbol{r}_m - \boldsymbol{p})}{|\boldsymbol{r}_m - \boldsymbol{p}|}}, \tag{9}$$

showing that the aircraft velocity $\boldsymbol{v}$ and position $\boldsymbol{p}$ can be determined by solving the system of equations defined by Eq. (9) for at least six independent pairs of microphones. This means that seven microphones are enough to obtain the aircraft position and velocity, $\boldsymbol{p}$ and $\boldsymbol{v}$. Here, all the possible pair combinations out of the seven microphones are considered to form a system of 42 nonlinear equations defined by Eq. (9), which is solved by using a genetic algorithm. The following least squares problem is stated

$$\min_{(\boldsymbol{p},\boldsymbol{v}) \in I} \sum_{m=1}^{N} \sum_{n \neq m} \left(\delta f_{mn} - \frac{c - \dfrac{\boldsymbol{v} \cdot (\boldsymbol{r}_n - \boldsymbol{p})}{|\boldsymbol{r}_n - \boldsymbol{p}|}}{c - \dfrac{\boldsymbol{v} \cdot (\boldsymbol{r}_m - \boldsymbol{p})}{|\boldsymbol{r}_m - \boldsymbol{p}|}} \right)^2 \tag{10}$$

where $I \subseteq \mathbb{R}^6$ is the search space for the three dimensional position and velocity of the aircraft. The kth iteration of the location algorithm gives $(\widehat{p_x^k}, \widehat{p_y^k}, \widehat{p_z^k}, \widehat{v_x^k}, \widehat{v_y^k}, \widehat{v_z^k}) \in I$ and the search space $I = [I_x, I_y, I_z, I_{v_x}, I_{v_y}, I_{v_z}] \subseteq \mathbb{R}^6$ is defined as follows:

$$I_u = \left[\widehat{p_u^{k-1}} - |v_{max,u}| \cdot \frac{\Delta t}{2}; \widehat{p_u^{k-1}} + |v_{max,u}| \cdot \frac{\Delta t}{2} \right] \tag{11a}$$

$$I_{v_u} = [v_{min,u}; v_{max,u}] \tag{11b}$$

where $u = x, y, z$ and $k > 0$.

The position and speed estimates obtained from solving the system of equations are then associated to the aircraft states at $k \cdot \frac{\Delta t}{2}$, i.e., $\boldsymbol{p}^k = \boldsymbol{p}(k \cdot \frac{\Delta t}{2})$ and $\boldsymbol{v}^k = \boldsymbol{v}(k \cdot \frac{\Delta t}{2})$.

Note however, that the Doppler stretch values δf_{mn} used to estimate each aircraft position are calculated using signal portions of length Δt. These stretch values correspond indeed to any time t within $[0; \Delta t]$ since Doppler stretches are not constant during Δt due to the continuous aircraft motion. Therefore, the estimated position obtained from that set of stretches can correspond as well to any position of the aircraft movement during Δt.

3. Experimental setup

The acoustic localization method described in section 2 is experimentally tested using a radio controlled airplane. The goal of this outdoor test is to compare the airplane trajectory estimated by the acoustic method and the trajectory given by a Global Positioning System (GPS) mounted on the airplane.

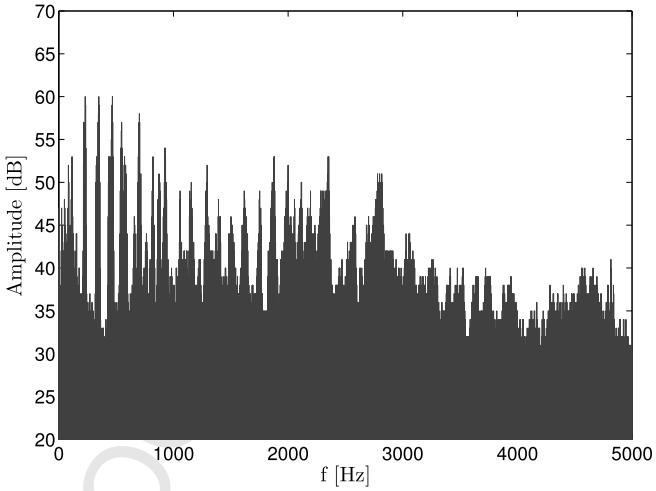

Fig. 2. The radio controlled airplane frequency spectrum.

3.1. Airfield

The experimental test has been carried out in the airfield of the Aeronautic Club Egara in Terrassa (Spain). It is placed at the outskirts of the city in an area where the background noise is low. It is not surrounded by any building that could introduce reflections of the sound emitted by the radio controlled airplane. The airfield is placed in a more or less rectangular flat area of 120 m long by 45 m wide of sandy soil. The runway is made of artificial grass and it is 72 m long by 15 m wide.

3.2. Radio controlled airplane

A radio controlled airplane with a 4-stroke engine has been used for the test. Fig. 2 shows the frequency spectrum of the airplane. The airplane was held while the engine was running (with the wheels not touching the ground) to record its spectrum with a microphone located 2 m far from the airplane. It can be seen from Fig. 2 that it is a tonal spectrum including multiples of the engine speed. Therefore, the frequency spectrum is highly dependent on the engine speed. The maximum speed of such an airplane is about 33 m/s.

3.3. Microphone distribution

To distribute the different microphones along the airfield, two different observations from the simulations published on [17] and [19] have been considered:

1. when the distance between the microphones is much smaller than the distance between the microphones and the source, the value of all the relative Doppler stretches δf_{mn} tends to the same value of 1 and the localization fails,
2. the higher the difference between all relative Doppler stretches, the higher the accuracy on the localization results.

Both remarks are directly dependent on the airplane trajectory. Therefore, to distribute the microphones accordingly, the airplane has been assumed to ideally fly-over along the runway at a constant altitude of 33 m, and a constant speed of 26 m/s (typical values for this particular kind of airplane). Note that this assumption is only used to select the positions of the sensors and should

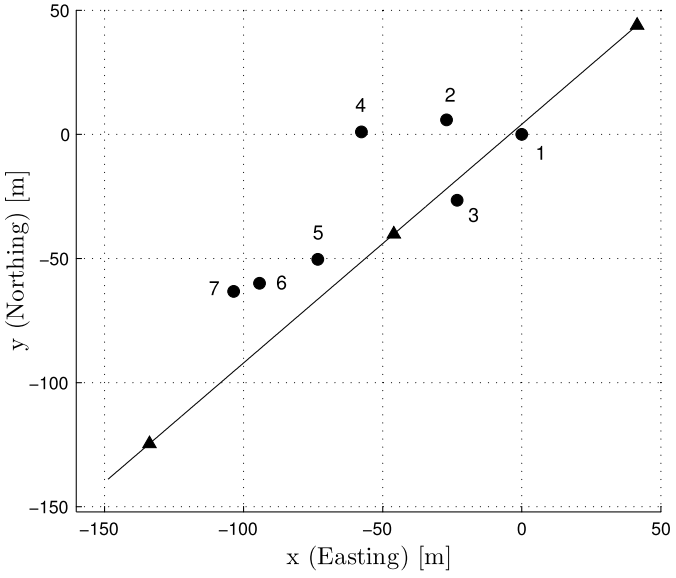

Fig. 3. Microphone distribution together with the expected aircraft trajectory which consists on fly-over at constant speed in one direction.

Table 1
Coordinates of each microphone $n \in \{1, \ldots, 7\}$ with the origin of coordinates set to the position of microphone 1.

n	1	2	3	4	5	6	7
r_{nx} (Easting) [m]	0	−27	−23	−58	−73	−94	−104
r_{ny} (Northing) [m]	0	6	−27	1	−51	−60	−54

not be interpreted as a movement restriction for the implementation of the acoustic method.

Fig. 3 shows the final microphone distribution together with this expected ideal airplane trajectory. The fly-over is considered to be in one direction at constant speed from the xy-point (41.08; 43.57) m to (−148.7; −138.9) m. Table 1 lists the microphones coordinates. The position of microphone 1 has been chosen to be the origin of coordinates.

According to the trajectory in Fig. 3, the evolutions of the absolute Doppler stretches δf_n for all microphones $n \in \{1, \ldots, 7\}$ are shown in Fig. 4. Fig. 4 shows that the absolute Doppler stretches δf_n for all microphones n are different enough up to $t = 8$ s.

Note that due to the small distances between the microphones themselves as well as the microphones and the radio controlled airplane, the experimental test carried out in this paper is a demanding test. The values of the absolute Doppler stretches are between 0.95 and 1.08 or equivalently, the values of the relative Doppler stretches are between $0.95/1.08 = 0.88$ and $1.08/0.95 = 1.13$ and this range is much smaller than the typical range obtained in a full scale application of the method which goes from 0.5 to 1.5 (see Ref. [19]).

3.4. Parameters

To initialize the acoustic location method, an initial position of the airplane $\boldsymbol{p}^{\text{initial}}$ at some time t^{initial} needs to be known. The coordinates of this initial position are given by the GPS mounted on the airplane. In the same system of coordinates than the microphone positions listed in Table 1, these airplane coordinates are $\boldsymbol{p}^{\text{initial}} = (41.4, 43.9, 35.1)$ m and the time corresponding to this position is set to $t^{\text{initial}} = 0$ s.

The sampling rate f_m needs to be chosen taking into account that the significant frequency content of the radio controlled airplane spectrum in Fig. 2 goes up to 2.5 kHz. Therefore, the sample

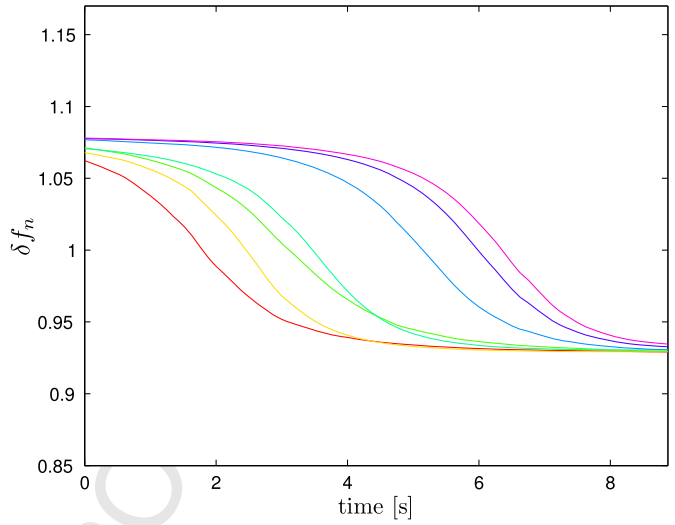

Fig. 4. Time evolution of the absolute Doppler stretches along the expected trajectory of the radio controlled airplane.

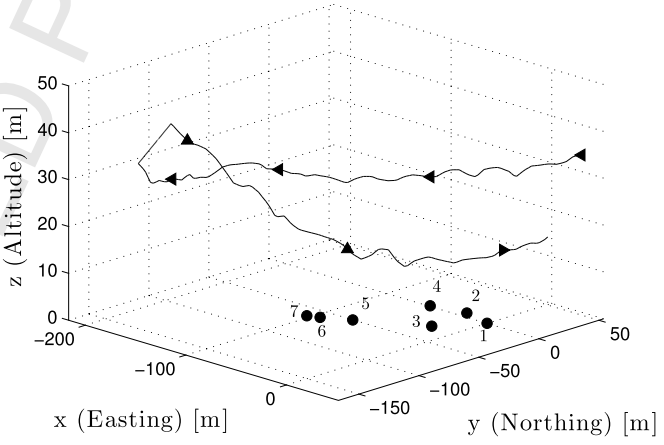

Fig. 5. Microphone distribution together with the radio controlled airplane trajectory provided by the GPS mounted on it.

frequency rate f_m for all microphones $n \in \{1, \ldots, 7\}$ has been of 5 kHz.

Regarding the time interval of the signal portions Δt, on the one hand, as said in Section 2, it has to be small enough so that the distance traveled by the airplane is much smaller than the distance between the airplane and the receiver and also so that the airplane velocity $\boldsymbol{v}$ can be considered a constant. On the other hand, it should be large enough to obtain an acceptable frequency resolution Δf when the Fourier Transform of the synchronized signals is computed. In the present test, the value $\Delta t = 0.15$ s satisfies all these conditions simultaneously.

Then, the frequency resolution of the Fourier Transform of all receivers signal is $\Delta f = 6.6$ Hz which is an acceptable resolution taking into account the frequency spectrum emitted by the airplane (Fig. 2). As a consequence of this choice, the acoustic method locates the radio controlled airplane every $\dfrac{\Delta t}{2} = 0.075$ s.

4. Results

This section presents the results for the acoustic localization of the radio controlled airplane. Fig. 5 shows the trajectory followed by the airplane during the experimental test provided by the GPS mounted on it. This trajectory will be named from now on *real* trajectory. It is worth remarking that the accuracy of the

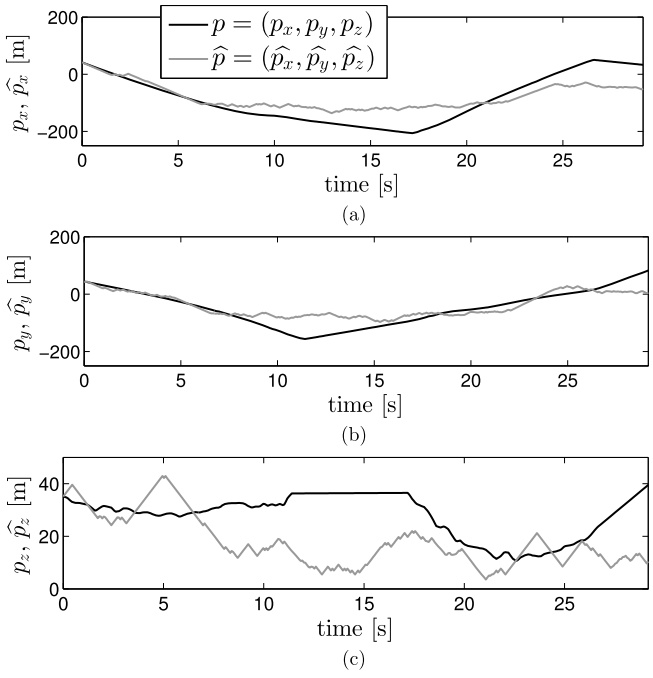

Fig. 6. Radio controlled airplane localization provided by the GPS ($p = (p_x, p_y, p_z)$) and estimated by the acoustic method ($\widehat{p} = (\widehat{p_x}, \widehat{p_y}, \widehat{p_z})$).

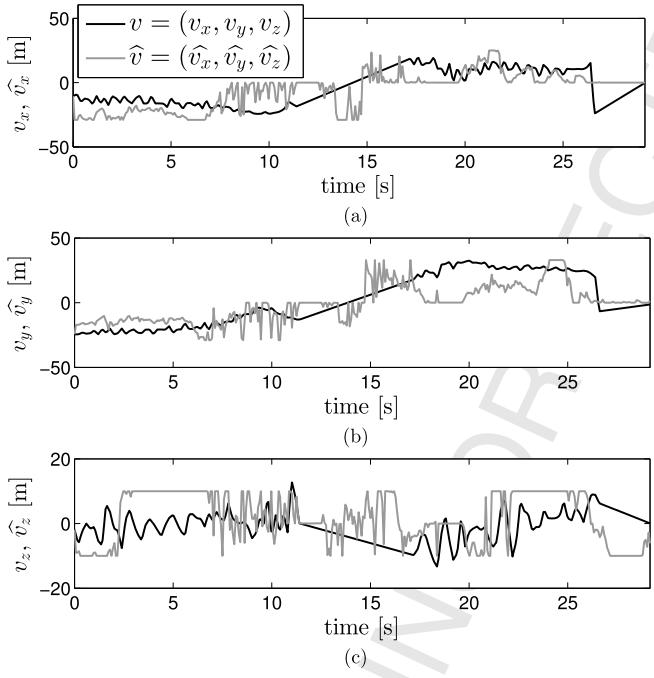

Fig. 7. Velocity of the radio controlled airplane provided by the GPS ($v = (v_x, v_y, v_z)$) and obtained from the acoustic method ($\widehat{v} = (\widehat{v_x}, \widehat{v_y}, \widehat{v_z})$).

GPS mounted above the radio controlled airplane is 3 m. Therefore what is called real position in the text is indeed an estimation of the real position with a 3 m accuracy. This uncertainty is disregarded in this paper and the real position is assumed to be an error-free result.

During the 30 s of signal analyzed here, the airplane flew over the runway in one direction for $t \in [0; 8]$ s, turned around sharply for $t \in]8; 18]$ s, and carried out a second fly-over in the opposite direction for $t \in]18; 30]$. The first fly-over is the main concern of discussion since the microphones have been distributed based on it (see section 3.3). Fig. 6 represents the estimated (obtained from

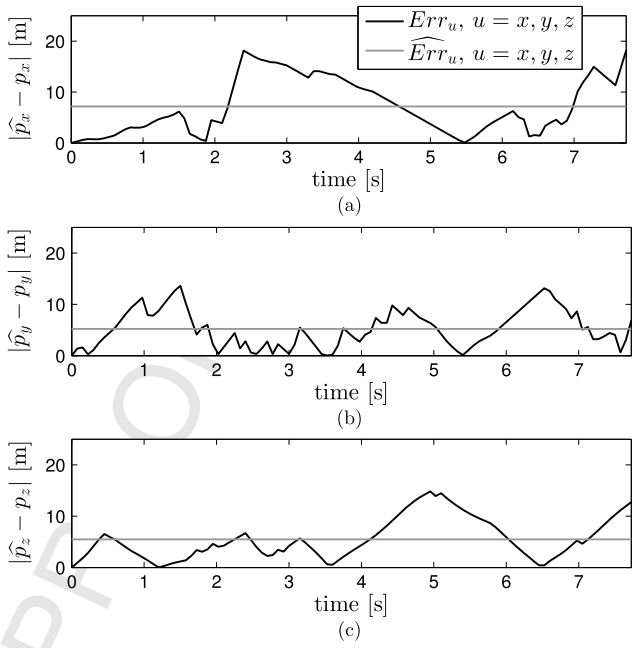

Fig. 8. Time evolution of the absolute localization error along the eight seconds fly-over for the three spatial coordinates: (a) x (Easting), (b) y (Northing) and (c) z (Altitude).

Table 2
Maximum and mean localization errors for each spatial coordinate x, y, z while $t \in [0; 8]$.

u	$\max(Err_u)$ [m]	$\widehat{Err_u}$ [m]
x	18.2	7.17
y	13.63	5.21
z	14.82	5.48

the acoustic method) and real positions of the airplane and Fig. 7 shows the estimated and real velocities. The gray curve in both figures corresponds to $\widehat{p} = (\widehat{p_x}, \widehat{p_y}, \widehat{p_z})$ and $\widehat{v} = (\widehat{v_x}, \widehat{v_y}, \widehat{v_z})$ which are the estimated airplane states provided by the acoustic method. The black curve corresponds respectively to $p = (p_x, p_y, p_z)$ and $v = (v_x, v_y, v_z)$ which are the real position and velocity provided by the GPS.

During the first fly-over for $t \in [0; 8]$ s, the radio controlled airplane flew along 210 m. Fig. 8 depicts the time evolution of the absolute error $Err_u = |\widehat{p_u} - p_u|$ where $\widehat{p_u}$ and p_u are the estimated and real airplane position respectively for each spatial coordinate $u = x, y, z$. Table 2 lists the maximum and mean errors for the time interval $t \in [0; 8]$ s, i.e., $\max(Err_u)$ and $\widehat{Err_u}$ where

$$\widehat{Err_u} = \frac{\sum_{k=1}^{K} |\widehat{p_u^k} - p_u^k|}{K}, \tag{12}$$

and K is the maximum number of executed iterations of the tracking algorithm.

Note that Fig. 8 shows that the maximum errors in Table 2 for each spatial coordinate are reached at different time instants and that the errors obtained are not cumulative. The acoustic method overcomes by itself these error peaks and tends to reach the real trajectory of the aircraft afterwards. Moreover, the mean error during 210 m of flight does not exceed 7.2 m in the x-coordinate and 5.5 m for both the y-coordinate and the altitude of the airplane. Section 5 focuses on this first fly-over and discusses different possible sources of this error.

For $t \in]8; 18]$ s when the airplane was turning sharply, the acoustic localization is not expected to be accurate since the setup has been optimized to locate the airplane during the first fly-over

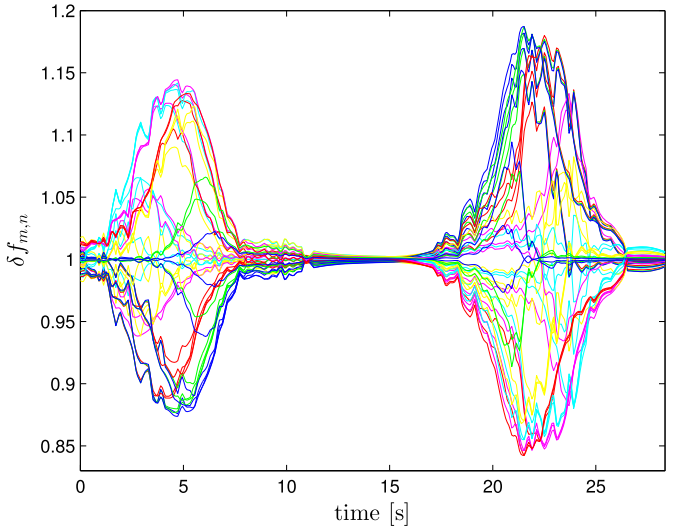

Fig. 9. Time evolution of the 42 values of relative Doppler stretches δf_{mn} for $m \neq n$, $m, n \in \{1, ..7\}$.

for $t \in [0; 8]$ (see section 3). Fig. 6 shows that both real and estimated locations differ the most. Actually, the Doppler effect does no longer affect in a different manner the signals received by the microphones. This means that $\delta f_{mn} = 1$ for all $m, n \in \{1, .., 7\}$ as can be seen in Fig. 9 that shows the time evolution of the 42 theoretical values of relative Doppler stretches during the flight.

Despite of the localization failure between $t = 8$ s and $t = 18$ s, the estimated position of the airplane tends to the real trajectory from $t = 18$ s onwards as shown in Fig. 6. The method seems to continue locating the airplane even if previously the localization has failed. Nevertheless, the error for $t \in [8; 18]$ s influences mainly the signals synchronization for $t > 18$ s (*Step 1* detailed in section 2) and thus, the accuracy of this second flyover is poorer.

Notice that this trajectory of the radio controlled airplane is not a common trajectory for a standard commercial aircraft when it approaches or leaves the airport. A full scale test of the acoustic localization method would not have two different directions of flight neither a sharp turn. This is why the discussion in section 5 focuses only on the first fly-over.

5. Discussion

The following section focuses on the results for $t \in [0; 8]$ introduced in section 4. This section discusses the influence of different sources of error such as the inherent error of the method due to the non-stop airplane motion during the time interval Δt (section 5.1), the sudden variation and uncertainty of the real position $\boldsymbol{p} = (p_x, p_y, p_z)$ (section 5.2), and the uncertainty of the exact positions of the microphones due to the inaccuracy of the GPS (section 5.3).

5.1. Influence of the continuous airplane motion

As detailed in section 2, each airplane position provided by the acoustic method is estimated by using signal portions of duration Δt. The estimated position is assigned to $\boldsymbol{p}(t^0 + \Delta t/2)$, but indeed this estimated position belongs to the spatial interval $[\boldsymbol{p}(t^0); \boldsymbol{p}(t^0 + \Delta t)]$ due to the continuous motion of the airplane during Δt. The maximum possible difference between $p_u(t^0)$ and $p_u(t^0 + \Delta t)$ for the spatial coordinates $u = x, y$ is at most $|v_{max}| \cdot \Delta t$. Thus, in this particular experimental test, the maximum inherent error of the acoustic method due to the airplane motion during Δt is $|v_{max}| \cdot \Delta t = 4.95$ m. This error can contribute significantly to the maximum errors in Table 2.

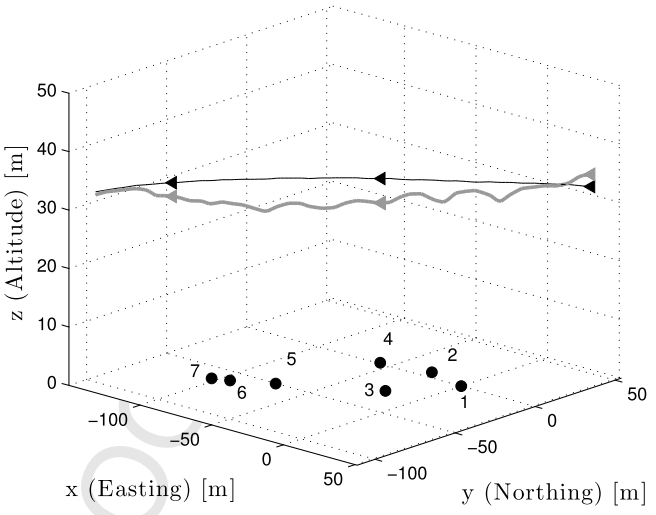

Fig. 10. Expected (in black) and real (in gray) trajectories of the radio controlled aircraft together with the distributed microphones.

5.2. Influence of the sudden variations in the real trajectory of the aircraft

Fig. 10 shows in gray color the airplane trajectory provided by the GPS and in black the expected trajectory. The real trajectory presents sudden oscillations that influence notably the value of the relative Doppler stretches.

Fig. 11 represents the time evolution of the 42 relative Doppler stretches used for localizing the airplane in flight considering the airplane travels along the real trajectory (Fig. 11a), and the expected trajectory (Fig. 11b) described in Section 3.3.

The acoustic localization method used here assumes that the Doppler stretches can be considered constant during Δt, but these sudden oscillations of the value of the relative Doppler stretches weaken this assumption introducing error in the estimates of the δf_{mn}. A wrong statement of the independent terms of the system of non-linear equations, i.e., δf_{mn} in Eq. (9), will lead to an inaccurate estimation of the airplane position.

5.3. Influence of the inaccuracy of the microphones positioning

The inaccuracy of the GPS used to obtain the microphone locations (an Etrex Venture by Garmin) is up to 3 m. To evaluate the influence of this uncertainty on the final position estimates, an error between 0 and 3 m has been randomly added to all receiver coordinates in Table 1. Then, the least squares problem stated in Eq. (10) has been solved using the real relative Doppler stretches showed in Fig. 11a, the real airplane trajectory in Fig. 10, and the microphone positions in Table 1.

Table 3 shows the averaged maximum localization error $\max(Err_u)$ and the mean localization error $(\widehat{Err}_u)$ obtained for each coordinate $u = x, y, z$ averaged over 100 realizations. Notice that the absolute error for each coordinate is calculated from the absolute value of the difference between the location estimation given by the acoustic method and the real trajectory given by the GPS mounted on the airplane which already contains an uncertainty of 3 m. The location errors from Table 3 are of the same order, even slightly higher, than those from Table 2. This result shows that the GPS inaccuracy that affects both the real position of the aircraft and the position of the microphones accounts for a substantial part of the total error. Notice that for the implementation of the method in an airport, the distances between microphones and aircraft will be of several kilometers and the GPS uncertainties will remain of 3 m. Therefore, the influence of the inaccuracy

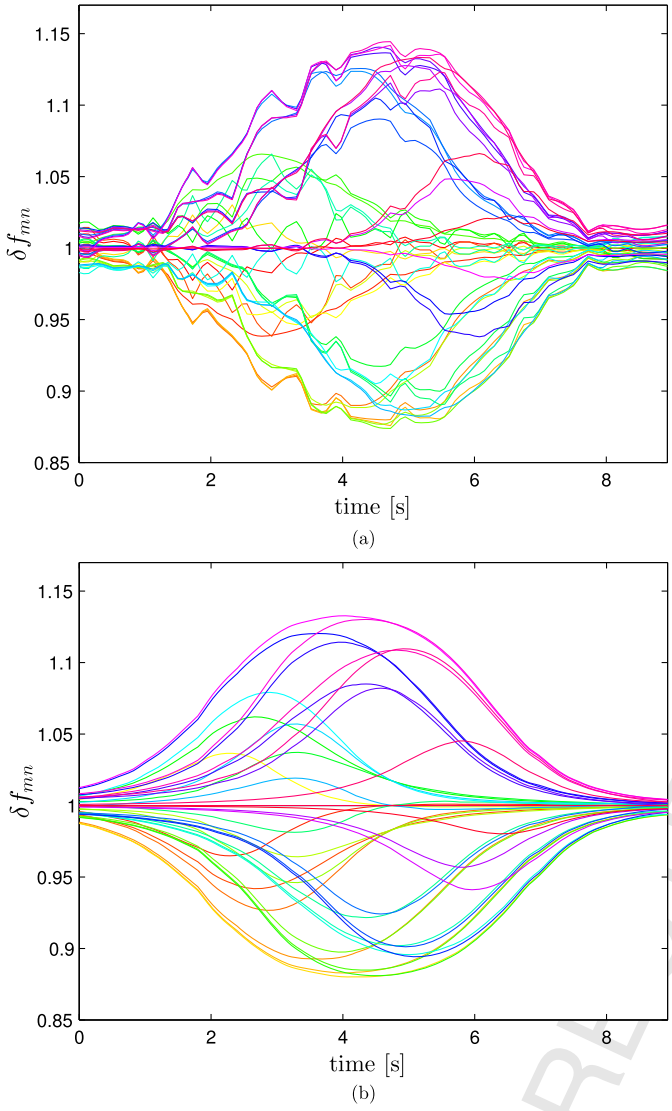

Fig. 11. Time evolution of the 42 relative Doppler stretches δf_{mn} for $m \neq n$, $m, n \in \{1, ..7\}$ computed from (a) the real and (b) expected trajectory of the airplane.

Table 3
Maximum and mean localization errors obtained using the real flyover of the airplane (Fig. 10) by randomly adding an error between 0 and 3 m to the microphone positions in Table 1.

u	$\max(Err_u)$ [m]	$\widehat{Err}_u$ [m]
x	19.9	8.1
y	18.2	7.2
z	12.7	4.6

of the microphones positions is not expected to affect as it does in the present reduced scale test.

6. Conclusions

The acoustic method for aircraft localization tested in this paper requires a simple set-up for its implementation in comparison with other location methods. The system needs basically a mesh of single microphones and does not require more complex structures such as microphones arrays or acoustic vector sensors to localize the aircraft. Furthermore, one of its main advantages is that the method is suitable for all kind of aircrafts. Based on the acoustical Doppler effect, the location system has no restrictions at all when it comes to the properties of the sound emitted by the aircraft.

An experimental test has been carried out using a radio controlled airplane and seven microphones distributed over the airfield area to validate the acoustic method. The main purpose of the test is to show the applicability of the acoustic localization method used. To do so the acoustically estimated airplane trajectory is compared to the trajectory provided by a Global Positioning System mounted on the airplane.

The present experiment is a highly demanding test and has several constraints. For instance, the 3 m uncertainty of the GPS devices used to locate both the radio controlled airplane and the set of seven microphones have a significant impact on the results taking into account the small distances between the sound source and receivers. Despite of these conditions, the localization errors provided by the acoustic method do not exceed the expected errors arising from the inaccuracy of the GPS devices used, but at the same time, their magnitude does not permit to quantify the exact error of the acoustic method. Therefore, it can be concluded that the method is capable of doing the measurements it has been developed for.

The experimental verification presented in this paper is a preliminary test of a full scale experiment. The influence of the different sources of errors discussed in this paper is expected to be notably smaller taking into account that the distances for a real scenario are at least 10 times longer and the velocity of the aircraft will be higher. Therefore, the results obtained in this experimental test are promising to move one step forward and test the acoustic method in an airport with commercial aircrafts.

Conflict of interest statement

None declared.

References

[1] B. Ferguson, A ground-based narrow-band passive acoustic technique for estimating the altitude and speed of a propeller-driven aircraft, J. Acoust. Soc. Am. 92 (3) (1992) 1403–1407, http://dx.doi.org/10.1121/1.403934.
[2] B. Ferguson, B. Quinn, Application of the short-time Fourier transform and the Wigner–Ville distribution to the acoustic localization of aircraft, J. Acoust. Soc. Am. 96 (2) (1994) 821–827.
[3] B. Fergusson, K. Lo, Turboprop and rotary-wing aircraft flight parameter estimation using both narrow-band and broadband passive acoustic signal-processing methods, J. Acoust. Soc. Am. 108 (4) (2000) 1763–1771.
[4] K. Lo, B. Ferguson, Flight path estimation using frequency measurements from a wide aperture acoustic array, IEEE Trans. Aerosp. Electron. Syst. 37 (2) (2001) 685–694.
[5] K. Lo, B. Ferguson, Broadband passive acoustic technique for target motion parameter estimation, IEEE Trans. Aerosp. Electron. Syst. 36 (1) (2000) 163–175, http://dx.doi.org/10.1109/7.826319.
[6] K. Lo, S. Perry, B. Ferguson, Aircraft flight parameter estimation using acoustical Lloyd's mirror effect, IEEE Trans. Aerosp. Electron. Syst. 38 (1) (2002) 137–151, http://dx.doi.org/10.1109/7.993235.
[7] K. Lo, B. Ferguson, Y. Gao, A. Maguer, Aircraft flight parameter estimation using acoustic multipath delays, IEEE Trans. Aerosp. Electron. Syst. 39 (1) (2003) 259–268, http://dx.doi.org/10.1109/TAES.2003.1188908.
[8] K. Lo, Flight parameter estimation using time delay and intersensor multipath delay measurements from a small aperture acoustic array, J. Acoust. Soc. Am. 134 (1) (2013) 17–28.
[9] H. Chen, J. Zhao, On locating low altitude moving targets using a planar acoustic sensor array, Appl. Acoust. 64 (11) (2003) 1087–1101.
[10] F. Dommermuth, J. Schiller, Estimating the trajectory of an accelerationless aircraft by means of a stationary acoustic sensor, J. Acoust. Soc. Am. 76 (4) (1984) 1114–1122.
[11] D. Dudgeon, Wideband array processing for acoustic detection and tracking of aircraft, in: Nineteenth Asilomar Conference on Circuits, Systems and Computers, 1985, pp. 263–266.
[12] F.M. Dommermuth, A simple procedure for tracking fast maneuvering aircraft using spatially distributed acoustic sensors, J. Acoust. Soc. Am. 82 (4) (1987) 1418–1424.
[13] R. Blumrich, J. Altmann, Medium-range localisation of aircraft via triangulation, Appl. Acoust. 61 (1) (2000) 65–82.

[14] M. Hawkes, A. Nehorai, Wideband source localization using a distributed acoustic vector-sensor array, IEEE Trans. Signal Process. 51 (6) (2003) 1479–1491.
[15] B.G. Fergusson, Time-delay estimation techniques applied to the acoustic detection of aircraft transits, J. Acoust. Soc. Am. 106 (1) (1999) 255–264.
[16] B.G. Fergusson, K. Lo, Turboprop and rotary-wing aircraft flight parameter estimation using both narrow-band and broadband passive acoustic signal-processing methods, J. Acoust. Soc. Am. 108 (4) (1999) 1763–1771.
[17] S.R. Martín, M. Genescà, J. Romeu, T. Pàmies, Aircraft tracking by means of the acoustical Doppler effect, Aerosp. Sci. Technol. 28 (1) (2013) 305–314.
[18] M. Genesca, J. Romeu, T. Pamies, A. Balastegui, Passive acoustic method for tracking moving sound sources, Acta Acust. Acust. 97 (1) (2011) 34–43.
[19] S.R. Martín, M. Genescà, J. Romeu, R. Arcos, Passive acoustic method for aircraft states estimation based on the Doppler effect, IEEE Trans. Aerosp. Electron. Syst. 50 (2) (2014) 1330–1346.

Please cite this article in press as: S.R. Martín et al., Aircraft localization using a passive acoustic method. Experimental test, Aerosp. Sci. Technol. (2015), http://dx.doi.org/10.1016/j.ast.2015.11.023